**International Global Navigation Satellite Systems Society**
**IGNSS Symposium 2013**

Outrigger Gold Coast, Qld Australia
16-18 July, 2013

# Quality Analysis of a Combined COMPASS/BeiDou-2 and GPS RTK Positioning Model

***Robert Odolinski (1)***
GNSS Research Centre, Curtin University of Technology, Australia
+61 8 9266 3157 & +61 8 9266 2703, email: robert.odolinski@curtin.edu.au
***Peter J.G. Teunissen (2)***
GNSS Research Centre, Curtin University of Technology, Australia, and Delft University of Technology, the Netherlands
+61 8 9266 7676 & +61 8 9266 2703, email: P.Teunissen@curtin.edu.au
***Dennis Odijk (3)***
GNSS Research Centre, Curtin University of Technology, Australia
+61 8 9266 3157 & +61 8 9266 2703, email: D.Odijk@curtin.edu.au

## ABSTRACT

The Chinese COMPASS/BeiDou-2 full constellation is expected by year 2020 with more than 30 satellites, and will provide global coverage. Australia is already a beneficiary of the regional Beidou system as enough satellites are available for Positioning, Navigation and Timing (PNT). A combined Beidou+GPS system increases the redundancy, which allows for higher accuracy and improved integrity. In this contribution we will compare a combined system performance with the Beidou- and GPS-only systems. The comparisons will involve integer ambiguity success rates and measures of precision of the estimated GNSS parameters and their reliability. Comparisons will involve single-frequency vs. multiple-frequencies and various satellite elevation cut-off angles. The results will show that the combined system allows for improved integer ambiguity success rates, satellite visibility and reliability as compared to the systems separately.

**KEYWORDS**: COMPASS/BeiDou-2, GPS, RTK, precision, variance matrix, reliability, Minimal Detectable Bias (MDB), integer ambiguity success rates

## 1. INTRODUCTION

The COMPASS satellite system, commonly known as BeiDou-2, attained initial regional operational status in the end of December 2011. Australia is a beneficiary of the current Beidou configuration located in the Asia-Pacific region, as enough satellites are available for Positioning, Navigation and Timing (PNT). Information about the navigation message was released to the public domain in December 2012 (CSNO, 2012). The full Beidou constellation is expected in 2020, and will consist of five Geostationary Earth Orbit (GEO), three Inclined Geo-Synchronous Orbit (IGSO) and 27 Medium Earth Orbit (MEO) satellites (CSNO, 2012). Beidou simulation results can be found in e.g. Grelier et al. (2007); Chen et al. (2009); Yang et al. (2011); Qu et al. (2012). Real data results were presented in Shi et al. (2012a) and Shi et al. (2012b) that evaluated Beidou-only Single Point Positioning (SPP), relative code

positioning, Real-Time-Kinematic (RTK), orbit determination and combined Beidou+GPS Precise Point Positioning (PPP). First real data Beidou results outside of China are reported in Montenbruck et al. (2012a, b) and Steigenberger et al. (2012, 2013). These later studies considered orbit determination, PPP, and single-baseline RTK positioning.

In this contribution we compare a combined system single-baseline RTK performance with the Beidou- and GPS-only systems. The comparisons will be made on measures of integer ambiguity success rates and on precision of the estimated GNSS parameters and their reliability. Reliability is a measure of robustness of the underlying model, and can be categorized into internal and external reliability. Internal reliability concerns the ability of the system to test the observations for modelling errors, and external reliability is referred to as the consequences on the estimated parameters when such model misspecifications are left undetected. For ambiguity resolution use is made of the LAMBDA method. The goal is to give Australian GNSS users indications of what Beidou can bring, both as a stand-alone system and when combined with GPS.

We start with a Beidou and GPS system overview, and describe the models and methods used for positioning and integer ambiguity resolution. Then we describe the reliability measures, and results are given. We conclude with a summary and discussion.

## 2. BEIDOU AND GPS FREQUENCIES AND WAVELENGTHS

The Beidou satellites currently transmit at three frequencies, B1, B2 and B3 in Quadrature phase-shift keying (QPSK) modulation as shown in Table 1, given together with the L1, L2 and L5 GPS frequencies. The Beidou signals are based on Code Division Multiple Access (CDMA) similar to GPS, Galileo and QZSS. We see that no Beidou frequencies overlap the GPS frequencies, and thus no Inter-system-bias parameterizations are needed (Odijk and Teunissen, 2013).

Table 1: COMPASS/BeiDou-2 and GPS signals.

| Sat. system | Band (component) | Frequency [ MHz ] | Wavelength [ cm ] |
|---|---|---|---|
| BEIDOU | B1 (I/Q) | 1561.098 | 19.20 |
| | B2 (I/Q) | 1207.140 | 24.83 |
| | B3 (I/Q) | 1268.520 | 23.63 |
| GPS | L1 | 1575.42 | 19.03 |
| | L2 | 1227.60 | 24.42 |
| | L5 | 1176.45 | 25.48 |

## 3. METHODOLOGY

This section briefly describes the float and fixed baseline least-squares solution and integer ambiguity resolution. Then we describe the internal and external reliability measures that will be analyzed in the results section.

### 3.1 Float and fixed baseline least-squares solution

In the following we describe how we solve our unknown parameters and the integer ambiguities. Consider a single-baseline RTK model and GNSS observations collected in the $m$-vector $y$, where we divide the unknowns into baseline components in vector $b$ including receiver position increments, receiver clock, etc., of say size $p \times 1$ with partial design matrix $B$, and (double-differenced) ambiguities in vector $a$ of size $q \times 1$ with design matrix $A$. We

will solve the following Integer Least-Squares (ILS) problem (Teunissen, 1995),

$$\min_{b,a} \| y - Bb - Aa \|^2_{Q_{yy}},\ b \in \mathbb{R}^p,\ a \in \mathbb{Z}^q \tag{1}$$

where $\| \cdot \|^2_{Q_{yy}} = (\cdot)^T Q_{yy}^{-1} (\cdot)$, $Q_{yy}$ is the GNSS observations' variance-covariance (VCV) matrix, $\mathbb{R}^p$ the $p$-dimensional space of real numbers and $\mathbb{Z}^q$ the $q$-dimensional space of integers. The parameter estimation is divided into three steps, *1)* float solution, *2)* integer ambiguity estimation, and *3)* fixed solution.

#### 3.1.1 Float solution

In the float solution we replace the integer constraint $\mathbb{Z}^q$ in (1) with $\mathbb{R}^q$, i.e. both the ambiguities and baseline components will be estimated as real-valued parameters. The unknown parameters can be solved by least-squares as follows (Teunissen et al., 2006),

$$\begin{bmatrix} \hat{b} \\ \hat{a} \end{bmatrix} = \begin{bmatrix} Q_{\hat{b}\hat{b}} & Q_{\hat{b}\hat{a}} \\ Q_{\hat{a}\hat{b}} & Q_{\hat{a}\hat{a}} \end{bmatrix} \begin{bmatrix} B^T Q_{yy}^{-1} y \\ A^T Q_{yy}^{-1} y \end{bmatrix} \tag{2}$$

$$\begin{bmatrix} Q_{\hat{b}\hat{b}} & Q_{\hat{b}\hat{a}} \\ Q_{\hat{a}\hat{b}} & Q_{\hat{a}\hat{a}} \end{bmatrix} = \begin{bmatrix} B^T Q_{yy}^{-1} B & B^T Q_{yy}^{-1} A \\ A^T Q_{yy}^{-1} B & A^T Q_{yy}^{-1} A \end{bmatrix}^{-1} \tag{3}$$

where $\hat{a}$, $\hat{b}$ are the least-squares solution of the ambiguities and baseline components respectively, and $Q_{\hat{a}\hat{a}}$, $Q_{\hat{b}\hat{b}}$, $Q_{\hat{a}\hat{b}}$ and $Q_{\hat{b}\hat{a}}$ are the corresponding (co-)variance matrices.

#### 3.1.2 Integer ambiguity estimation

It can be shown that the integer solution of (1) is given by the integer minimizer,

$$\breve{a} = \underset{a \in \mathbb{Z}^q}{arg\ min} \| \hat{a} - a \|^2_{Q_{\hat{a}\hat{a}}} \tag{4}$$

which can efficiently be computed with the LAMBDA method (Teunissen, 1995). The ILS estimator in the LAMBDA method results in the highest possible success rates of all integer estimators (Teunissen et al., 1996, Teunissen 1999, 2002).

#### 3.1.3 Fixed baseline solution

The fixed baseline solution $\breve{b}$ of the (integer) constrained linear model (Teunissen et al., 2006) then reads,

$$\breve{b} = \hat{b} - Q_{\hat{b}\hat{a}} Q_{\hat{a}\hat{a}}^{-1} (\hat{a} - \breve{a}) \tag{5}$$

If we neglect the uncertainty in $\breve{a}$, the corresponding VCV-matrix is given as,

$$Q_{\breve{b}\breve{b}} = Q_{\hat{b}\hat{b}} - Q_{\hat{b}\hat{a}} Q_{\hat{a}\hat{a}}^{-1} Q_{\hat{a}\hat{b}} \tag{6}$$

The uncertainty in $\breve{a}$ can be neglected if the probability of correct integer estimation is sufficiently high. Ensuring that the used integer ambiguity solution has a sufficiently high probability of being correct is the task of integer validation, see e.g. the Fixed Failure rate Ratio Test (FFRT) in (Teunissen and Verhagen, 2009), and (Verhagen and Teunissen, 2012).

### 3.2 Reliability, detection and identification of outliers

Reliability is a measure of robustness of the underlying model. We consider the following two composite hypotheses (Teunissen et al., 2006),

$$H_0 : E(y) = Ax, \tag{7}$$

and,

$$H_a : E(y) = Ax + C_y \nabla \tag{8}$$

In the null hypothesis $H_0$ in (7) we have $E(.)$ as the expectation operator, $y$ as the $m$-vector

of observations, $A$ the $m \times n$ (full-rank) design matrix and $x$ the $n$-vector of unknowns. Further in the alternative hypothesis $H_a$ in (8) we have $C_y$ as an $m \times q$ (full-rank) matrix relating the outliers in the $q$-vector $\nabla$ ($\nabla \neq 0$) to the observations $y$, where $1 \leq q \leq m-n$. In the absence of outliers (7) should be taken to estimate the unknown parameters $x$, otherwise (8). We emphasize that $A$ should not be confused with the one in equation (1), i.e. the design matrix now also contains columns for the baseline components in addition to the ambiguities.

In order to describe the relevance of internal and external reliability, we need to introduce the Detection, Identification and Adaptation (DIA) procedure that can be used to identify and eliminate outliers (Teunissen, 1990). We focus on the Detection and Identification steps.

#### 3.2.1 Detection

The Detection step in the DIA procedure concerns testing the model in (7) for all kinds of errors on all observations without any specific error signature in mind, i.e. it considers a full $C_y$ in (8) of size $q$=$m$-$n$. The test statistic used is referred to as the Local Overall Model (LOM) test, see (Teunissen et al., 2006), and follows a central F-distribution with $m-n, \infty$ degrees of freedom (Figure 1). If the LOM test is exceeding a critical value as defined by a lookup table of the F-distribution for a certain level of significance, the Identification step should be taken since our assumed model in (7) then might be affected by outliers or anomalies.

#### 3.2.2 Identification

Identification concerns constructing the $C_y$ matrix in (8) to identify, if any, outliers $\nabla$. Since many different alternative hypotheses can be taken, we usually restrict us to the case of one outlier per observation $q = 1$ for practical applications. Hence we formulate $m$ number of alternative hypotheses by $m$ number of $c_{y_i}$ canonical vectors in (8), i.e. a vector of size $m \times 1$ with a 1 at the $i$:th position, with $i = 1,2,\ldots,m$, and the remaining zeros. This way of screening the observations is referred to as data snooping (Baarda, 1968), and can be tested by the so called w-test statistic, see (Teunissen et al., 2006). The w-test is standard normally distributed under $H_0$ (Figure 1).

#### 3.2.3 Minimal Detectable Bias and internal reliability

Reliability of the LOM and w-test can be controlled by the power of test $\gamma$, i.e. the probability of rejecting $H_0$ in (7) when the alternative hypothesis $H_a$ (8) is indeed true. The power of the test is a function of $\alpha$ the level of significance, i.e. the probability of rejecting $H_0$ when it is true (false alarm), the number of degrees of freedom $q$, and the non-centrality parameter $\lambda$. By fixing the power of the tests we can make sure that both tests detect a certain size of a bias with the same probability. Recall this probability as $\gamma_0$, and the non-centrality parameter $\lambda_0$ can then be fixed according to the following inverse power-function (Baarda, 1968),

$$\lambda_0 = \lambda(\alpha, m-n, \gamma_0) = \lambda(\alpha_0, 1, \gamma_0) \tag{9}$$

This implies that if we fix the power of the test for both the LOM and w-test, and as well fix $\alpha_0$ for the w-test, we achieve the same size of the non-centrality parameter and thus same reliability for both tests. This quantity can for the F-distributed LOM-test and the normally distributed w-test be considered as an offset between the two modes of the corresponding distributions, see Figure 1.

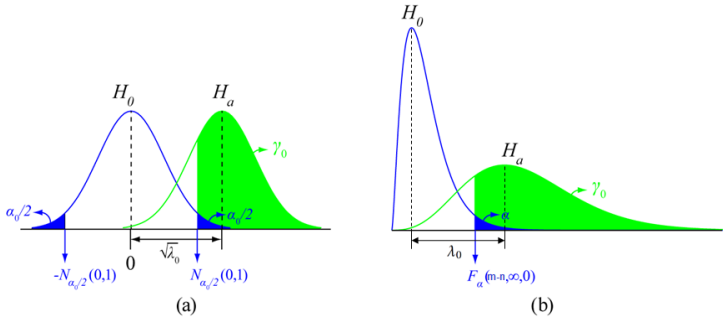

Figure 1: Linking the power of the LOM and w-test as well as the non-centrality parameter.

From this non-centrality parameter one can already in the design stage, before taking actual measurements, compute the Minimum Detectable Bias (MDB). We have $\lambda = \nabla^T c_y^T Q_{yy}^{-1} Q_{\hat{e}\hat{e}} Q_{yy}^{-1} c_y \nabla$ as the non-centrality parameter for the one-dimensional outlier case, with $Q_{yy}$ as the observations' VCV-matrix, $Q_{\hat{e}\hat{e}} = P_A^{\perp} Q_{yy} P_A^{\perp T}$ as the VCV-matrix of the least-squares residuals and $P_A^{\perp} = \left(I_m - A\left(A^T Q_{yy}^{-1} A\right)^{-1} A^T Q_{yy}^{-1}\right)$ as a projector that projects onto the orthogonal complement to the range space of $A$. We then get,

$$|\nabla| = \sqrt{\frac{\lambda_0}{c_y^T Q_{yy}^{-1} Q_{\hat{e}\hat{e}} Q_{yy}^{-1} c_y}} \tag{10}$$

as the MDB (Teunissen, 1998a). One can also besides the MDB consider the following scalar squared Bias-to-Noise Ratio (BNR), with a specific outlier in $\nabla y = c_y \nabla$ in case of data snooping,

$$\lambda_y = \nabla y^T Q_{yy}^{-1} \nabla y \tag{11}$$

A small value of $\lambda_y$ indicates that the bias is small as compared to the observation noise, whereas a large value indicates that the bias is significantly large.

#### 3.2.4 External reliability

We can then compute the impact the bias $\nabla y$ has on the estimated unknown parameters $\hat{x}$ as obtained by taking (7), when (8) is actually true. The probability that the bias is not detected is also referred to as the probability of missed detection $1\text{-}\gamma_0$. With the bias propagation law and the difference of the hypotheses in (7) and (8) given as $E(y|H_a) - E(y|H_0) = \nabla y = C_y \nabla$, we get,

$$\nabla \hat{x} = (A^T Q_{yy}^{-1} A)^{-1} A^T Q_{yy}^{-1} \nabla y \tag{12}$$

This vector $\nabla \hat{x}$ represents the impact a bias in $\nabla y$ will have on the least-squares estimates under the null hypothesis (7) in case of a missed detection. We can also compute the squared BNR for the unknown parameters, similar to (11), as,

$$\lambda_{\hat{x}} = \nabla \hat{x}^T Q_{\hat{x}\hat{x}}^{-1} \nabla \hat{x} \tag{13}$$

where $Q_{\hat{x}\hat{x}} = (A^T Q_{yy}^{-1} A)^{-1}$ is the VCV-matrix of the unknown parameters. It can be shown (Teunissen, 2006) that the relation between $\lambda_y$, $\lambda_0$ and $\lambda_{\hat{x}}$ is,

$$\lambda_{\hat{x}} = \lambda_y - \lambda_0 \tag{14}$$

In other words, once the internal BNR (11) has been computed, the external BNR follows by subtracting the non-centrality parameter (9) from equation (11).

## 4 RESULTS

Data from one static receiver CUTA in Curtin's Continuously Operating Reference Stations and one experimental receiver CUTT are evaluated. The stations are equipped with Trimble NetR9 multi-frequency multi-GNSS receivers. One day of data was processed, namely April 21, 2013, with 30 sec interval between consecutive measurements. The distance between the stations is approximately 964 m. The Beidou (CSNO 2012) and GPS satellite orbits and clocks are given by the broadcast ephemerides. The estimated receiver positions are compared to very precise station benchmarks, and we make use of the DIA procedure to detect, identify and adapt for outliers. The CUTA antenna is shown to the left of Figure 2, whereas CUTT is given to the right. Typical skyplot, number of satellites and Positional Dilution Of Precision (PDOP) for a combined Beidou+GPS system is given in Figure 3 for April 21, UTC +0 hours. We see in Figure 3 that the current Beidou constellation overall provides us with a larger number of satellites over the day as compared to GPS.

Figure 2: CUTA (Left) and CUTT (Right) GNSS antennas, baseline distance 964 m.

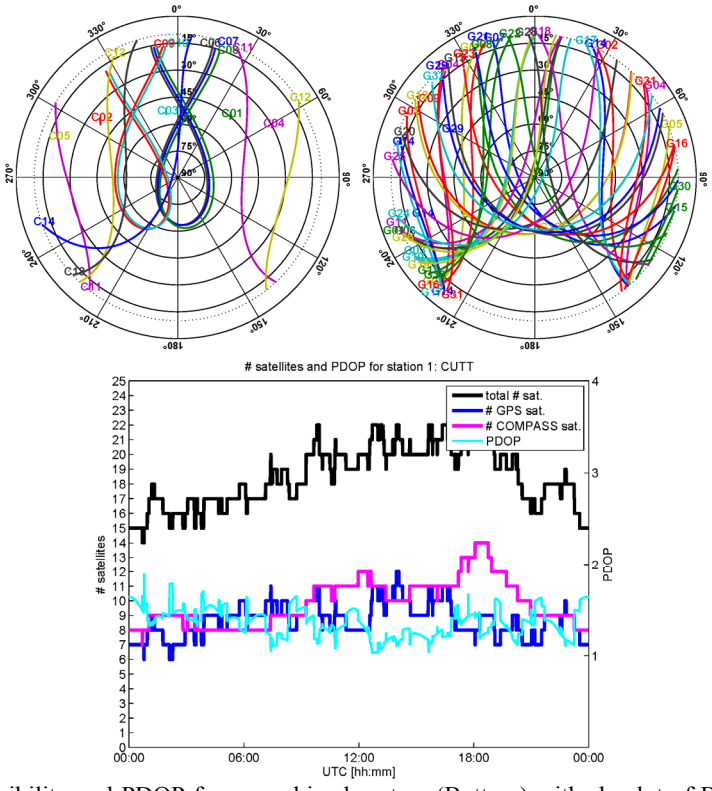


Figure 3: Satellite visibility and PDOP for a combined system (Bottom) with skyplot of Beidou (Top left) and GPS (Top right), with **10 degrees** elevation cut-off angle for CUTT in Perth and April 21, 2013.

### 4.1 Single-baseline RTK stochastic settings

The stochastic model settings in $Q_{yy}$ for single-baseline RTK positioning are given in Table 2. We used data from other days than presented in this contribution to find these settings. We then applied these settings to the daily data to be analyzed to independently check the validity of the stochastic model used. The stochastic model is the exponential elevation weighting function as defined in (Euler and Goad, 1991). We restrict our analyses to Beidou B1 and B2 frequencies (not B3) to fairly compare the results to dual-frequency GPS L1 and L2.

Table 2: Stochastic model settings for single-baseline RTK, with a priori standard deviations for code and phase.

| Sat. system | Frequency | Code [ cm ] | Phase [ mm ] |
|---|---|---|---|
| BEIDOU | B1 | 31 | 2.5 |
| | B2 | 30 | 3.3 |
| GPS | L1 | 37 | 2.5 |
| | L2 | 27 | 2.6 |

### 4.2 Single-baseline RTK positioning results

Single-frequency RTK positioning results are shown in Figure 4 with epoch-by-epoch (instantaneous) integer ambiguity resolution for 10 degrees elevation cut-off angle and a combined B1+L1 Beidou+GPS system. Only the correctly fixed solutions are shown at bottom as determined by comparing the ambiguities to a set of reference ambiguities, see the description in relation to equation (15). Horizontal and vertical scatter plots are given with 95% confidence ellipses/levels derived from the empirical and formal VCV-matrix of the positions. The empirical VCV-matrix is given by the positioning errors as obtained from comparing the estimated positions to precise benchmark coordinates. The benchmark coordinates for our experimental receiver CUTT was obtained by using a combined Beidou+GPS RTK-system with multiple frequencies. The formal VCV-matrix is given from the mean of all single-epoch formal VCV-matrices of the entire observation span. All results are given in local North, East and Up and local Perth time, UTC +8 hours. A good match between the two ellipses implies realistic assumptions on the stochastic model and that we as a result have a minimum variance estimator (Teunissen et al., 2006).

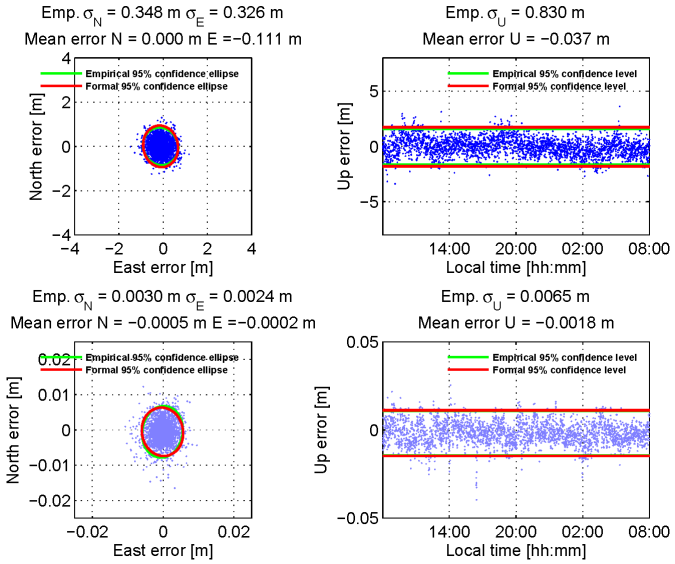


Figure 4: B1+L1 combined Beidou+GPS single-epoch and single-baseline RTK positioning scatter for CUTA-CUTT and April 21, 2013 and **10 degrees** cut-off angle. Float solutions (Top) and fixed solutions (Bottom), where empirical positioning mean errors and standard deviations are given in local North, East and Up.

We see in Figure 4 a good match between the formal and empirical ellipses/confidence levels, which implies that we have realistic stochastic settings in Table 2. We also see that the precision of the float solutions go from dm-meter level, down to a few mm standard deviations for the fixed solutions.

### 4.3 Integer ambiguity success rates and time-to-fix

The success rate, i.e. the probability of correct integer estimation, cannot be computed exactly for ILS. Fortunately however, the so called bootstrapped success rate can be used as an accurate lower bound to the ILS success rate (e.g. Teunissen, 1997, 1998b). We will denote this probability as $P_{s,B}$. This success rate can be computed without actual measurements i.e. only the (decorrelated) VCV-matrix (Teunissen, 1995) of the float ambiguities is needed.

We can also compute the so called ILS empirical success rates by comparing the estimated ambiguities to reference ambiguities. These reference ambiguities are estimated by using a combined Beidou+GPS system over the whole time-span with multiple-frequencies and a Kalman filter, assuming the ambiguities time-constant. The empirical success rate is given as,

$$P_{s_E} = \frac{\#\text{correct integer amb.}}{\text{total}\,\#\text{of integer amb.}} \tag{15}$$

The empirical failure rate is given as the complement,

$$P_{f_E} = 1 - P_{s_E} \tag{16}$$

#### 4.3.1 Single-epoch success rates for various elevation cut-off angles

Empirical ILS success, failure and bootstrapped success rates for elevation cut-off angles ranging between 10-35 degrees are given in Table 3 for single- and multiple-frequency RTK. The higher elevation cut-off angles are taken as to mimick conditions with obstructed satellite availability such as in urban canyons or open pit mines. The bootstrapped success rates are computed as the mean of all single-epochs over the day. We denote all success rates of 100% with bold and in green color, whereas non-zero failure rates are denoted with red color.

The bootstrapped success rates in Table 3 are indeed good lower bounds to the ILS solutions, except for the combined system B1+L1 (98.1% vs. 100%) that is related to some epochs with poor quality signals from low elevation satellites (see e.g. a 15 degree cut-off angle, where the empirical success rate instead reach 100%). As expected the single-frequency single-system with the largest code noise (Table 2), smallest wavelength (Table 1) and number of satellites (Figure 3), also give the highest fractions of empirical failure rates (GPS L1). All epochs were however successfully fixed for all elevation angles for the combined-system when using multiple-frequencies. The GPS single-frequency system performs considerably worse than Beidou due to the smaller number of visible satellites at high elevations (see e.g. Figure 5). Very promisingly though is that the single-frequency combined system gives close to 100% success rates for elevation cut-off angles up to 30 degrees, and even 97%-98% at an elevation cut-off angle of 35 degrees. Compare these numbers to Beidou- and GPS-only success rates, with values down to 9% for GPS L1 and 52% for Beidou B1, and 35 degrees.

#### 4.3.2 The wrongly fixed solutions single-epoch positioning results

For a surveyor collecting measurements in real-time, reference ambiguities are usually not available beforehand. This is where integer validation plays an important role (Teunissen and Verhagen, 2009). In Figure 5, B1 Beidou, L1 GPS and B1+L1 combined positioning results, with an elevation cut-off angle of 35 degrees, are given. The float solution is given in gray, correctly fixed solution in green, and the wrongly fixed solutions in red. We also give at bottom the number of satellites equal/above and below 8 for a single-system, and 9 for a

combined system, and the corresponding bootstrapped success rates (SR). The number of satellites lower bound for the combined system is set to 9 due to parameterization of different receiver clocks between the systems (one additional unknown). The GPS clock is given with respect to GPS time and the Beidou clock to BeiDou navigation satellite system time (CSNO, 2012). Gaps are seen in the GPS results since less than 4 satellites are visible for these epochs and thus the receiver coordinates are not (unbiased) estimable.

Table 3: Empirical ILS success, failure and bootstrapped success rates for single- and multiple-frequency RTK, CUTA-CUTT and elevation cut-off angles of **10, 15, 20, 25, 30 and 35 degrees** (from left to right respectively). Number of epochs 2880 (30 sec interval).

| **System/ frequency** | **Empirical Success rate** $P_{s_E}$ [%], cut-off [deg] | | | | | | **Failure rate** $P_{f_E}$ [%], cut-off [deg] | | | | | | **Bootstrapped Success rate** $P_{s,BS}$ [%], cut-off [deg] | | | | | |
|---|---|---|---|---|---|---|---|---|---|---|---|---|---|---|---|---|---|---|
| | 10 | 15 | 20 | 25 | 30 | 35 | 10 | 15 | 20 | 25 | 30 | 35 | 10 | 15 | 20 | 25 | 30 | 35 |
| BEIDOU | | | | | | | | | | | | | | | | | | |
| B1 | 96.4 | 96.1 | 86.9 | 83.4 | 66.8 | 51.5 | 3.6 | 3.9 | 13.1 | 16.6 | 33.2 | 48.5 | 93.1 | 92.8 | 80.7 | 77.1 | 60.0 | 42.4 |
| B2 | 97.6 | 97.5 | 87.5 | 84.6 | 72.6 | 59.4 | 2.4 | 2.5 | 12.5 | 15.4 | 27.4 | 40.6 | 96.0 | 95.8 | 86.9 | 83.7 | 67.1 | 52.1 |
| GPS | | | | | | | | | | | | | | | | | | |
| L1 | 79.4 | 68.9 | 52.6 | 33.4 | 19.3 | 9.0 | 20.6 | 31.1 | 47.4 | 66.6 | 80.7 | 91.0 | 67.9 | 54.8 | 37.8 | 21.4 | 11.0 | 4.4 |
| L2 | 93.3 | 87.3 | 73.5 | 50.6 | 32.5 | 16.9 | 6.7 | 12.7 | 26.5 | 49.4 | 67.5 | 83.1 | 90.0 | 82.3 | 67.3 | 45.6 | 28.3 | 14.5 |
| COMBINED | | | | | | | | | | | | | | | | | | |
| B1+L1 | 98.1 | **100** | **100** | **100** | 99.4 | 97.0 | 1.9 | 0.0 | 0.0 | 0.0 | 0.6 | 3.0 | **100** | **100** | **100** | 99.9 | 98.7 | 94.4 |
| B2+L2 | **100** | **100** | **100** | **100** | 99.7 | 97.6 | 0.0 | 0.0 | 0.0 | 0.0 | 0.3 | 2.4 | **100** | **100** | **100** | **100** | 99.6 | 97.5 |
| BEIDOU | | | | | | | | | | | | | | | | | | |
| B1,B2 | **100** | **100** | **100** | **100** | 99.9 | 99.7 | 0.0 | 0.0 | 0.0 | 0.0 | 0.1 | 0.3 | **100** | **100** | **100** | **100** | 99.8 | 98.9 |
| GPS | | | | | | | | | | | | | | | | | | |
| L1,L2 | **100** | **100** | **100** | 99.1 | 97.6 | 96.0 | 0.0 | 0.0 | 0.0 | 0.9 | 2.4 | 4.0 | **100** | **100** | 99.9 | 98.2 | 94.8 | 90.4 |
| COMBINED | | | | | | | | | | | | | | | | | | |
| B1,B2+L1,L2 | **100** | **100** | **100** | **100** | **100** | **100** | 0.0 | 0.0 | 0.0 | 0.0 | 0.0 | 0.0 | **100** | **100** | **100** | **100** | **100** | **100** |

In Figure 5 we see that the correctly fixed positioning errors are very small (mm-level), and the Figure illustrates well the need of integer validation since the wrongly fixed solutions standard deviations become even larger than the corresponding values for the float solutions (meter-level). The number of satellites above/equal 8 (single-system) and 9 (combined-system) is shown to be a good indication whether single-frequency integer ambiguity resolution can be successful. This number of satellites (for 35 degree cut-off angle) is, however, only available approximately 18% of the time for Beidou and *never* for GPS, whereas 9 satellites (or more) are available approximately 92% of all epochs for the combined system. The insufficient number of satellites is also reflected in the float and wrongly fixed positioning results, particularly for GPS with errors of several tens of meters in the Up component. We see more specifically six large peaks of the Up errors that are related to poor satellite geometry, thus we depict the number of satellites and PDOP for GPS in Figure 6. By inspecting Figure 6 we have indeed PDOP peaks at the same time as for the float and wrongly fixed solutions in Figure 5. This implies that the combined system does not only dramatically improve the success rates (from 9% L1 GPS and 52% B1 Beidou, to 97% empirical success rate for a combined system), but also the satellite geometry and positioning availability.

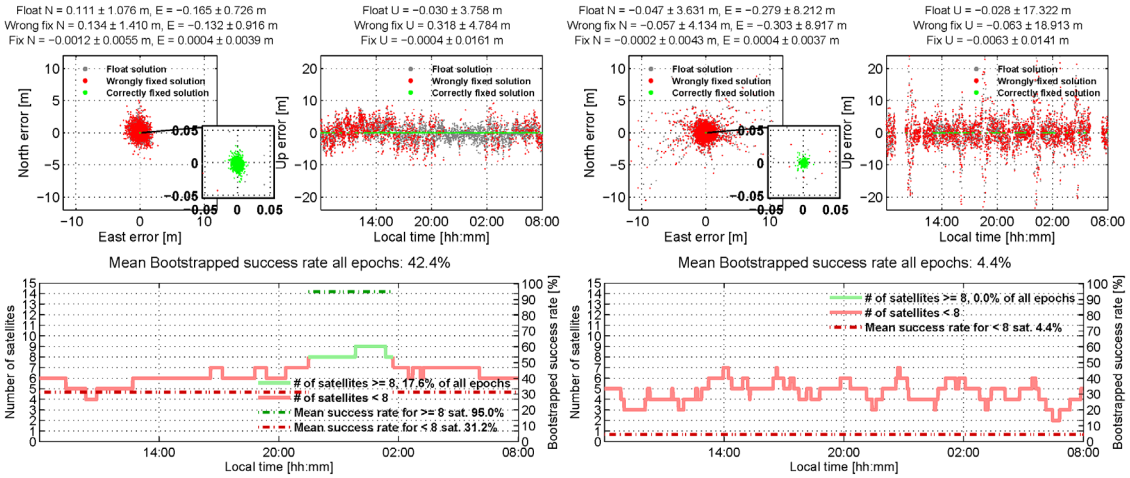


(a) B1 Beidou positioning and bootstrapped SR (35 deg). (b) L1 GPS positioning and bootstrapped SR (35 deg).

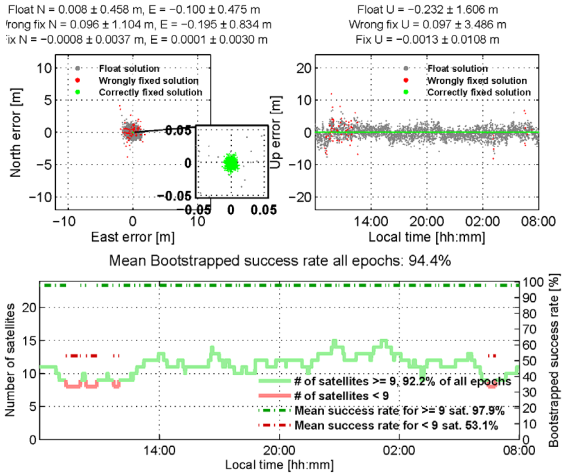


(c) B1+L1 Combined positioning and bootstrapped SR (35 deg).

Figure 5: Float (gray), correctly fixed (green) and wrongly fixed (red) solutions for single-epoch single-baseline RTK B1 Beidou (a), L1 GPS (b), and combined B1+L1 (c) positioning scatter for CUTA-CUTT and an elevation cut-off angle of **35 degrees**. Mean positioning errors ± standard deviations given in local North, East and Up. At the bottom of each positioning scatter plot light green represents number of satellites above or equal 8 (9 for combined) satellites, red corresponding color is for below 8 (9 for combined) satellites. Bootstrapped success rates are taken as a mean of all epochs above/equal and below these satellite limits.

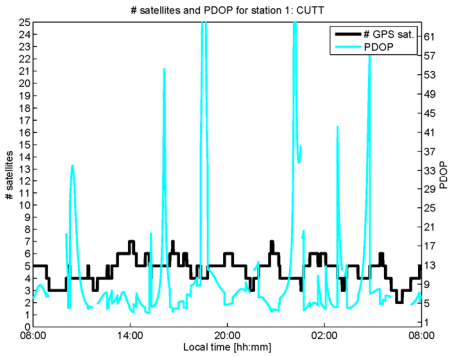


Figure 6: PDOP and number of satellites for GPS and an elevation cut-off angle of **35 degrees**.

### 4.3.3 Time-to-fix for single-frequency solutions

We conclude this section by giving the most demanding RTK scenario with single-frequency data and elevation cut-off angle of 35 degrees, but now instead of epoch-by-epoch solutions

we accumulate epochs by a Kalman filter assuming the ambiguities time-constant. This procedure goes as follows; The filter is initialized (at the first epoch) and based on the (filtered) set of float ambiguities, integer ambiguity resolution is attempted. The fixed ambiguities are then compared to the true reference ambiguities, and if they are not correct another epoch is included in the filter, and so on, until the estimated integer ambiguities are correct. When this is true, the filter is re-initialized at the second epoch, and the whole process is repeated again. In this way it is decided how many epochs that are needed for successful ambiguity resolution (time-to-fix). The time-to-fix results with mean ± standard deviation over the day are depicted in Figure 7 for B1 Beidou, L1 GPS and a B1+L1 combined system. Gaps are again seen in the GPS results since less than 4 satellites are visible for these epochs (Figure 6).

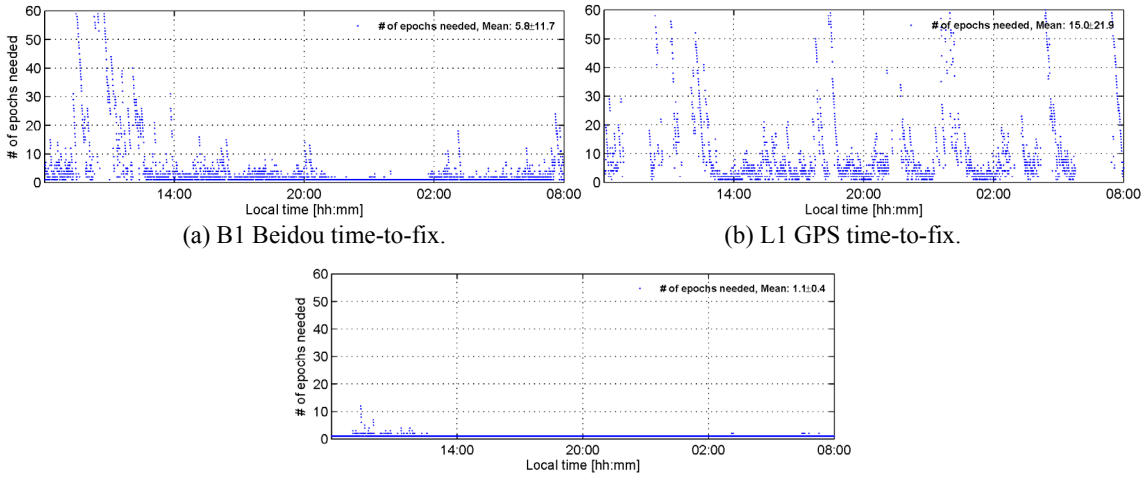


(a) B1 Beidou time-to-fix. (b) L1 GPS time-to-fix.

(c) B1+L1 combined time-to-fix.

Figure 7: Time-to-fix (1 epoch = 30 sec) with mean ± standard deviation over the day for an elevation cut-off angle of **35 degrees** and single-baseline RTK B1 Beidou (a), L1 GPS (b) and B1+L1 combined (c) for CUTA-CUTT.

The combined system needs (estimated as a mean value) 1.1 epochs for successful ambiguity resolution, with a standard deviation of 0.4 epochs. Corresponding value for the single-systems are approximately 6 epochs (3 min) for Beidou B1 (standard deviation 6 min), and 15 epochs (7.5 min) for GPS L1 (standard deviation 11 min). When comparing Figure 7 to Figure 5, we see overall that the number of required epochs is one (instantaneous ambiguity resolution) when the number of satellites is sufficient (equal/above 8/9 satellites). This holds true for most of the epochs from approximately 9/10 p.m. to slightly before 2 a.m. local Perth Time for Beidou, and at all times for the combined system, except for some epochs before 12 a.m. For GPS however the number of satellites *never* reaches the sufficient number of satellites and thus we need (for 91% of the time, see Table 3) more than one epoch to successfully fix the ambiguities.

### 4.4 Internal and external reliability

The robustness of the GPS, Beidou and combined models against model errors is analyzed for single-frequency RTK. Two types of model errors have been assumed: i) outliers in the code data, and ii) cycle-slips in the phase data. Outliers affect the code observations of one single epoch, while cycle-slips shift the phase observations from a certain epoch by an integer amount of cycles. For both types of model errors we compute code outlier and phase slip MDBs and BNRs in a systematic way (by data snooping) for all observations during the day. While the code outlier MDBs/BNRs can be computed based on one single epoch, the phase

slip MDBs/BNRs are based on two consecutive epochs, for which the ambiguities are treated as time constant between them. The BNRs are taken as the square root of equation (13). We computed MDBs and BNRs as daily mean values for each satellite. In Table 4 and 5 we present the ranges (minimum to maximum) of these daily means for all satellites. In order to make a comparison between the 10-degree (Table 4) and 35-degree (Table 5) cases possible, the MDB time series time-span, from which the per-satellite mean MDB was computed, was in both cases confined to the 35-degree cut-off angle. The redundancy will however still be different between scenarios, since (other) visible satellites below 35 degrees are also contributing in the 10-degree case. In other words, we expect larger values of MDBs/BNRs in the 35-degree case, due to the less redundancy as compared to the 10-degree case. The MDBs are computed based on a significance level of 0.001 and a power of 0.80, such that the non-centrality parameter is 17.07. Large deviating values of MDBs/BNRs are given within brackets.

Table 4: Range of daily mean of code outlier (single-epoch) and phase slips (two-epochs) MDBs/BNRs for single-frequency B1 Beidou, L1 GPS, and B1+L1 combined, for an elevation cut-off angle of **10 degrees**.

| **Model** | **System/ frequency** | **Code outlier (1 epoch)** | | **Phase slip (2 epochs)** | |
|---|---|---|---|---|---|
| | | **MDB [m]** | **BNR** | **MDB [cyc]** | **BNR** |
| SINGLE-SYSTEM | BEIDOU B1 | 2-5 | 6-8 | 0.07-0.2 | 0.2-0.8 |
| | GPS L1 | 3-4 | 6-8 | 0.08-0.1 | 0.3-1.1 |
| COMBINED | BEIDOU B1 | 2-3 | 5-8 | 0.07-0.08 | 0.2-0.4 |
| | GPS L1 | 2-3 | 5-6 | 0.07-0.09 | 0.2-0.8 |

Table 5: Range of daily mean of code outlier (single-epoch) and phase slips (two-epochs) MDBs/BNRs for single-frequency B1 Beidou, L1 GPS, and B1+L1 combined, for an elevation cut-off angle of **35 degrees**.

| **Model** | **System/ frequency** | **Code outlier (1 epoch)** | | **Phase slip (2 epochs)** | |
|---|---|---|---|---|---|
| | | **MDB [m]** | **BNR** | **MDB [cyc]** | **BNR** |
| SINGLE-SYSTEM | BEIDOU B1 | 2-24 | 5-76 | 0.08-1.1 (some MDBs > 9) | 0.3-0.8 (some BNRs > 100) |
| | GPS L1 | 4-38 | 10-160 | 0.2-9.0 (some MDBs > 15) | 0.9-110 (some BNRs > 1000) |
| COMBINED | BEIDOU B1 | 2-4 | 6-8 | 0.07-0.1 | 0.2-0.5 (some BNRs > 10) |
| | GPS L1 | 3-4 | 6-8 | 0.08-0.1 | 0.3-0.9 (some BNRs > 6) |

It can be seen from Table 4 that with a cut-off of 10 degrees the code outliers MDBs lie in the range of 2-5 m for Beidou-only and 3-4 m for GPS-only. The Beidou MDBs are generally smaller than those of GPS, because of the lower noise of the Beidou B1 code data (see Table 2) and (on average) the larger number of Beidou satellites tracked (see Figure 3). The corresponding BNRs are in the range of 6-8 for both Beidou and GPS. When the constellations are combined the values for the code outlier MDBs/BNRs are decreased as compared to the single-system MDBs/BNRs, this since the combined model is stronger and has higher redundancy. The phase slip MDBs lie in the range of 0.07-0.2 cycles for Beidou-only and 0.08-0.1 cycles for GPS-only. These are slightly improved in the combined solution to values ranging between 0.07-0.09 cycles. The corresponding BNRs, which are up to 0.8 for Beidou-only and up to 1.1 for GPS-only, are also slightly improved when the two are combined.

The results using the much higher cut-off elevation of 35 degrees are as follows. From Table 5 it can be seen that the mean code outlier MDBs are in the range of 2-24 m for Beidou, and those for GPS in the range of 4-38 m. These much larger ranges as compared to the 10-degree

cut-off scenario are due to the low redundancy when using a 35 degree cut-off angle (see Figure 5). The corresponding single-system BNRs can take on very large values as well: up to 160 for GPS. In other words, the reliability becomes poorer when we decrease the number of satellites. A significant improvement in code outlier robustness can however be observed for a combined Beidou+GPS system: the MDBs reduce to low values below 4 m and the BNRs are not larger than 8 for both systems. With an elevation cut-off angle of 35 degrees, the phase slip MDBs can also be very large: MDBs larger than 9 cycles are observed for Beidou-only and even larger values (more than 15 cycles) for GPS-only. This implies that cycle slips smaller than these values may not be detected, which can inhibit (non-instantaneous) integer ambiguity resolution. This is also visible from the corresponding BNR values, which can be more than 100 for Beidou-only and even more than 1000 for GPS-only. However, the results improve significantly when the two constellations are combined: all phase slip MDBs become at most 0.1 cycles, while the corresponding BNR has some sporadic outliers of 10 at most. By comparing the 35-degree MDBs/BNRs for the combined system with the corresponding 10-degree, we see a much less degradation of the reliability as compared to the single-system cases. This is promising, since a combined system does then not only allow for high success rates for large elevation angles (Table 3), but also preserves the reliability of the model.

## 5. CONCLUSIONS

In this contribution we have studied the third satellite system Beidou that in addition to GPS and GLONASS provides continuous PNT in the Asia-Pacific region. We focused our attention on positioning in Perth, Western Australia and a combined Beidou+GPS single-baseline RTK model, the integer ambiguity success rates and the internal/external reliability of the model. The comparisons were made to the systems separately. We can summarize our findings and conclusions as follows.

### 5.1 Integer ambiguity success rates for various satellite elevation cut-off angles

In Table 3 we summarized (single-epoch) ILS empirical success rates results for single- and multiple-frequency Beidou, GPS and combined Beidou+GPS RTK. This was given for several different satellite cut-off elevation angles (10-35 degrees), where higher cut-off angles are suitable in e.g. urban canyons or open pit mines. Our main conclusion is that with an elevation cut-off angle of up to 35 degrees, a combined single-frequency Beidou+GPS system can provide us with empirical success rates of 97%-98%. The corresponding number for 30 degrees was 100%. If we compare the 35 degree results to the single-systems, with success rates ranging between 9% (for L1 GPS) to at most 59% (for B2 Beidou), it is indeed a dramatic and promising improvement. We also concluded that the Beidou-only system currently has, during a 24 hour period, more satellites at higher elevation angles as compared to GPS and with respect to our receivers, which allows for larger Beidou success rates for different cut-off angles.

### 5.2 Time-to-fix

When looking into the most demanding scenario with an elevation cut-off angle of 35 degrees and single-frequency (B1 and L1) data, we found by using a Kalman filter that the time-to-fix was (almost) only one epoch for the combined system, taken as mean over the day. The corresponding numbers for Beidou and GPS were 6 epochs (3 min) and 15 epochs (7.5 min) respectively (Figure 7). The time-to-fix results were also found to be correlated to the number of satellites as depicted in Figure 5, and the corresponding (single-epoch) bootstrapped success rates.

### 5.3 Internal and external reliability

When the constellations were combined, the values of the code outlier MDBs/BNRs were slightly decreased for a 10 degree of elevation cut-off angle (Table 4), with a significant improvement for the 35 degree angle (Table 5). More specifically, in the latter case the code MDBs were decreased from several tens of meters down to a few meters. With an elevation cut-off angle of 35 degrees, the single-system phase slip MDBs also become very large. We obtained MDBs larger than 9 cycles for Beidou, and more than 15 cycles for GPS. This implies that cycle slips smaller than these values might not be detected for a single-system, which can seriously inhibit (non-instantaneous) integer ambiguity resolution. However, the results improve significantly when the two constellations are combined, where all phase slip MDBs become at most 0.1 cycles, while the corresponding BNR has some sporadic outliers of 10. Comparing 35-degree MDBs/BNRs (Table 5) with the corresponding 10-degree results (Table 4), we can also conclude that a combined system preserves the reliability of the model.

Beidou has already been shown to be suitable as a complementary or standalone GNSS system for Australia. More satellites are upcoming and will improve the Beidou and combined Beidou+GPS system even further.

## ACKNOWLEDGEMENTS

This work has been executed in the framework of the Positioning Program Project 1.01 "New carrier phase processing strategies for achieving precise and reliable multi-satellite, multi-frequency GNSS/RNSS positioning in Australia" of the Cooperative Research Centre for Spatial Information (CRC-SI). The second author is the recipient of an Australian Research Council (ARC) Federation Fellowship (project number FF0883188). Data was provided by Noor Raziq and Boris Padovan, and help was provided from Nandakumaran Nadarajah with the Beidou navigation message, all at the GNSS Research Centre of Curtin University. All this support is gratefully acknowledged.

## REFERENCES

Baarda, W. (1968) A testing procedure for use in geodetic networks. Netherlands Geodetic Commission, Publ. on Geodesy, New Series, 2(5), 1968.

Chen, H.C., Huang, Y.S., Chiang, K.W., Yang, M. and Rau, R.J. (2009) The performance comparison between GPS and BeiDou-2/COMPASS: A perspective from Asia. *J. of the Chinese institute of engineers*, 32(5):679–689, 2009.

CSNO (2012). BeiDou Navigation Satellite System Signal In Space Interface Control Document by China Satellite Navigation Office (CSNO). Open service signal B1I (Version 1.0). Technical report, December 2012. 77 pages., 2012.

Euler, H. J. and Goad, C. g. (1991) On optimal filtering of GPS dual frequency observations without using orbit information. *Bulletin Geodesique*, 65:130–143, 1991.

Grelier, T., Ghion, A., Dantepal, J., Ries, L., DeLatour, A., Issler, J-L., Avila-Rodriguez, JA., Wallner, S. and Hein, GW. (2007) Compass signal structure and first measurements. In *Proc. of ION GNSS-2007*, pages 3015–3024, Fort Worth, TX, September 2007.

Montenbruck, O., Hauschild, A., Steigenberger, P., Hugentobler, U., Teunissen, P.J.G. and Nakamura, S. (2012a) Initial assessment of the COMPASS/BeiDou-2 regional navigation satellite system. *GPS Solutions*, 2012. DOI 10.1007/s10291-012-0272-x.

Montenbruck, O., Hauschild, A., Steigenberger, P., Hugentobler, U. and Riley, S. (2012b) A COMPASS for Asia: First experience with the BeiDou-2 Regional Navigation System. In *Proc. of IGS Workshop 2012, July 23-27, Olsztyn, Austria*, 2012.

Odijk, D. and Teunissen, P.J.G. (2013) Characterization of between-receiver GPS-Galileo

inter-system biases and their effect on mixed ambiguity resolution. *GPS Solutions*, Springer-Verlag, p. 1-13, DOI 10.1007/s10291-012-0298-0, 2013.

Qu, J., Yuan, H., Zhang, X. and Ouyang, G. (2012) Single-epoch COMPASS carrier-phase ambiguous resolution using three civil frequencies and special constellations. In *25th ITM of the Satellite Division of the Institute of Navigation, Nashville TN, September 17-21*, 2012.

Shi, C., Zhao, Q., Li, M., Tang, W., Hu, Z., Lou, Y., Zhang, H., Niu, X. and Liu, J. (2012a) Precise orbit determination of Beidou Satellites with precise positioning. *Science China Earth Sciences*, 55:1079–1086, 2012. doi: 10.1007/s11430-012-4446-8.

Shi, C., Zhao, Q., Hu, Z. and Liu, J. (2012b) Precise relative positioning using real tracking data from COMPASS GEO and IGSO satellites. *GPS Solutions*, pages 1–17, 2012. DOI 10.1007/s10291-012-0264-x.

Steigenberger, P., Hauschild, A., Hugentobler, U. and Montenbruck, O. (2012) Performance analysis of Compass orbit and clock determination and Compass only PPP. In *Proc. of IGS Workshop 2012, July 23-27, Olsztyn, Austria*, 2012.

Steigenberger, P., Hugentobler, U., Hauschild, A., Montenbruck, O., (2013). Orbit and clock analysis of COMPASS GEO and IGSO satellites. *J. of Geodesy* doi:10.1007/s00190-013-0625-4.

Teunissen, P. J. G. (1990) An integrity and quality control procedure for use in multi sensor integration. In *Proc. of the* $3^{rd}$ *ITM of the Satelllite Division of the Institute of Navigation (ION GPS 1990)*, pages 513–522, Colorado Spring, CO, September 1990. Also published in: Volume VII of the GPS Red Book Series: Integrated systems, *ION Navigation*, 2012.

Teunissen, P. J. G. (1995) The least squares ambiguity decorrelation adjustment: a method for fast GPS integer estimation. *J. of Geodesy*, 1995. 70: 65-82.

Teunissen, P. J. G. (1997) A canonical theory for short GPS baselines. Part IV: Precision versus reliability. *J. of Geodesy*, 1997. 71: 513-525.

Teunissen, P. J. G. (1998a) Minimal detectable biases of GPS data. *J. of Geodesy*, 1998. 72: 236-244.

Teunissen, P. J. G. (1998b) Success probability of integer GPS ambiguity rounding and bootstrapping. *J. of Geodesy*, 1998. 72: 606-612.

Teunissen, P. J. G. (1999) An optimality property of the integer least-squares estimator. *J. of Geodesy*, 1999. 73: 587-593.

Teunissen, P. J. G. (2002) The parameter distributions of the integer GPS model. *J. of Geodesy*, 2002. 76: 41-48.

Teunissen, P. J. G. (2006). Testing theory - an introduction. Series on Mathematical Geodesy and Positioning, Delft University of Technology, 2006, The Netherlands.

Teunissen, P. J. G., de Jonge, P.J., and Tiberius, C.C.J.M. (1996) The volume of the GPS ambiguity search space and its relevance for integer ambiguity resolution. *Proc. of ION GPS*. Volume 9, pages 889-898, 1996.

Teunissen, P. J. G., Simons, D.G. and Tiberius, C.C.J.M. (2006) Probability and Observation Theory. *Lecture Notes AE2-E01, Delft University of Technology, The Netherlands*, 2006.

Teunissen, P. J. G. and Verhagen, S. (2009) The GNSS ambiguity ratio-test revisited: a better way of using it. *Survey Review Vol. 41, No. 312*, pages 138–151, 2009.

Verhagen, S. and Teunissen, P. J. G. (2012) The ratio test for future GNSS ambiguity resolution. *GPS Solutions*, 2012. DOI 10.1007/s10291-012-0299-z.

Yang, Y.X., Li, J.L., Xu, J.Y., Tang, J., Guo, H.R. and He, H.B. (2011) Contribution of the Compass satellite navigation system to global PNT users. *Chinese Science Bulletin*, 56(26):2813–2819, 2011.